

Soft segment composition and its influence on phase-separated morphology of PCL/PEG-based poly(urethane urea)s

Fatemeh Shokrolahi · Hamid Yeganeh

Received: 30 July 2013 / Accepted: 17 April 2014 / Published online: 8 May 2014
© Iran Polymer and Petrochemical Institute 2014

Abstract A composition-dependent microphase separation of segmented poly(urethane urea)s (PUUs), based on a mixture of two hydrophobic (polycaprolactone) and hydrophilic (polyethylene glycol) polyols, is investigated. Synthesis of PUUs was carried out through the reaction of in situ generated AB-type macromonomers, prepared from the reaction of NCO-terminated urethane prepolymers, with benzoic acid in dimethyl sulfoxide as solvent/reagent at 40–80 °C. The segmented PUUs were characterized by different methods including FTIR and NMR spectroscopies, gel permeation chromatography, differential scanning calorimetry and dynamic mechanical analysis. Microphase separation in the synthesized PUUs was monitored using atomic force microscopy (AFM) to find a better insight into structure–property relationship of PUUs consisting of mixed polyols. Thermal analysis of the polymers revealed that by introducing poly(ethylene glycol) (PEG) in PUU backbone, a well-defined glass transition was obtained. The results of AFM showed that PCL-based poly(urethane urea) has a morphology in which hard segment domains were homogeneously distributed in the soft segment matrix. In the samples based on PCL/PEG, the hard segment domains aggregates were connected to each other and were inhomogeneously distributed in the matrix. Comparison of the overall data revealed that the differences in soft segment compositions had a marked effect on the molecular structure and the mechanical properties of PUUs.

Keywords Poly(urethane) urea · Phase domain · Microphase separation · Atomic force microscopy

Introduction

Over the last few years, segmented polyurethanes (PUs) have received considerable attention because of offering a combination of biodegradability, elastomeric properties and thermoplastic processing conditions, which make them potential candidates for novel applications, especially in tissue engineering and medical devices [1–3]. In contrast to traditional elastomers, these thermoplastic elastomers owe their unique mechanical properties to the presence of thermoreversible cross-linkages. The segmented PUs which contain alternating soft and hard segments may suggest unique possibilities of tailor-made polymers by varying block length and composition. The block with a glass transition temperature below zero is known as soft segment and it is usually a polyester or polyether and the second block is recognized as hard segment [4, 5]. The phase-separated structure and two-phase morphology in these segmented block copolymers are due to thermodynamic immiscibility between the hard and soft segments. Parameters such as volume fractions, chemical composition, molecular weight and molecular weight distribution of each segment have great influence on physically cross-linked network behavior and mechanical properties of PUs and polyureas as well as their microphase-separated structure. Therefore, the study of the degree of microphase separation between the hard and soft segments in poly(urethane urea)s (PUUs), based on mixed soft segments, plays a key role in better understanding of the mechanical behavior of PUUs.

The microphase segregation of segmented PUs has been studied by a variety of characterization techniques, including dynamic mechanical analysis (DMA) and differential scanning calorimetry (DSC) [6–8], infrared spectroscopy [9, 10] and small-angle X-ray scattering

F. Shokrolahi (✉) · H. Yeganeh
Iran Polymer and Petrochemical Institute, P.O. Box: 14965/115,
Tehran, Iran
e-mail: f.shokrolahi@ippi.ac.ir

(SAXS) [11]. Recently, in numerous research works, atomic force microscopy (AFM) has been found to be an important tool for demonstrating the influence of hard and soft segments structural nature [8, 12, 13] as well as their molecular weights [14–16] on the microphase-separated structure of segmented polymers.

Some parameters such as differences in segments length and composition are effective on interfacial interaction of polyurethane system. Hydrogen bonding plays very critical roles in specification of the morphology and properties of PUs and poly(urethane ureas). Wilkes et al. [17] compared the morphology of highly branched polyurethane urea copolymers with their linear analogs for the microstructure characterization using AFM phase imaging technique. In their studies, a variety of morphologies were shown for hard segments including disordered, particulate and short rod-like domains. In another study, they accomplished the morphological analysis of non-chain extended PUs and polyureas [18]. The polymers showed phase-separated morphologies with thread-like crystalline hard segments dispersed in a continuous soft segment matrix.

Recently, we have reported a straight forward and versatile method for the preparation of thermoplastic segmented non-chain extended PUUs based on polycaprolactone (PCL) [19]. Despite appropriate mechanical properties of PCL soft segment-based PUs for tissue engineering applications, they provide high hydrolytic stability and, therefore, very low hydrolytic degradation rate under biological condition. The biodegradation rate of PUs is typically controlled by the nature of soft segment structure. A common practice to control the degradation profile of PUs and PUUs is to take advantage of a strongly hydrophilic co-polyol, such as poly(ethylene glycol) (PEG) to render the polymer more hydrophilic and consequently more prone to hydrolytic degradation [20–22].

In continuation of our previous work, some partial replacement of PCL with PEG was conducted and the properties and microstructure of the resulting PUUs were studied with respect to their corresponding structural modifications. The hard segment content was kept constant to investigate just the impact of changes in degree of hydrogen bonding on morphology by introducing ether groups, which create weaker hydrogen bonds in comparison to ester groups (the ratio of polyol:diisocyanate was constant and the molecular weights of PEG and PCL were about 4,000). The morphology of the samples was studied using AFM. The aim of this work was to monitor the structure–property relationships of segmented PUUS as a function of PCL/PEG weight ratio using AFM. To the best of our knowledge, this is the first report on microphase segregation in PUUs based on mixed PCL/PEG polyols of equal molecular weights.

Experimental

Materials

PCL ($\overline{M}_n = 4,155$ Da) from Solvay Chemicals (CAPA[®]240, US) was dried at 80 °C under vacuum for 24 h. PEG ($\overline{M}_n = 3,937$ Da) from Aldrich (US) was partially dried under vacuum at 80 °C for 48 h. Hexamethylene diisocyanate (HDI) from Merck (Germany) was used as received. Benzoic acid from Merck (Germany) was freed from absorbed moisture by storing in a vacuum oven at 60 °C for 5 h. Dimethyl sulfoxide (DMSO) from Merck (Germany) was distilled over CaH₂ under reduced pressure and stored on 0.4 nm molecular sieve.

Characterization

Verification of the chemical structure of the PUUs was performed in transmission and reflection modes with a Fourier transform infrared spectrometer (FTIR, ATR, Bruker, Germany). The molecular weights of the polymers were measured by an Agilent 1100 modular gel permeation chromatography system, equipped with a refractometer index (RI) detector. Solutions of the samples, each containing 1 mg/mL PUUs, were prepared in chloroform and the molecular weights were measured against polystyrene standards.

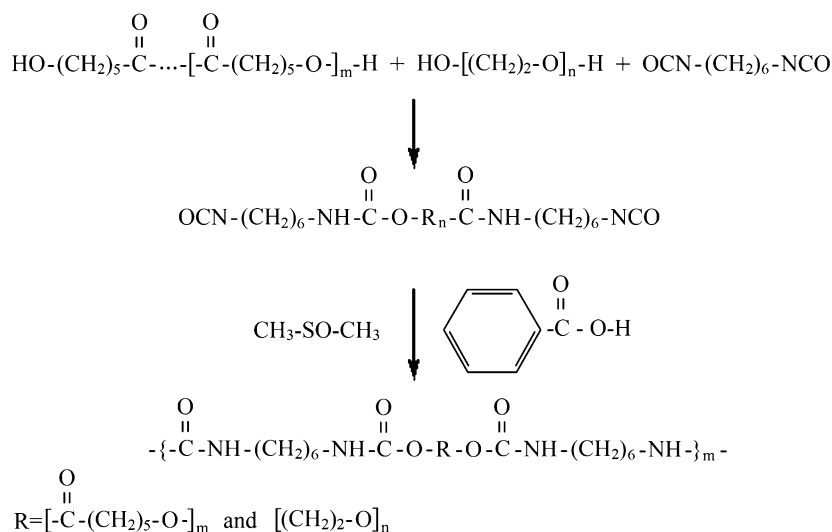
Densities of the synthesized polymers were measured according to the test method reported in ASTM D 1817 using a six-column density measuring apparatus.

The wettability of the PUUs films was determined by measuring contact angles ($n = 7$) of distilled water on polymer surfaces using sessile drop method on a Kruss model contact angle goniometer (Hamburg, Germany).

DSC measurements were carried out on a 200 F3 machine, Netzsch, Germany. Cyclic DSC measurements were performed on 10–12 mg samples with scanning rate of 10 °C/min over a temperature range of –100 to 130 °C under nitrogen atmosphere. The reported data were taken from second heating run.

Dynamic mechanical behavior of the polymers was investigated on a Triton 2000 DMA instrument from –100 to 80 °C at a heating rate of 4 °C/min and frequency of 1 Hz on samples of 10 × 10 × 1 mm³.

Phase structure of the PUU films was studied on an AFM based on Dual Scope 95-200E scanner (tapping etched silicon probe) type single beam cantilevers. This technique allowed simultaneous detection of height and degree of phase segregation. The spring constant was 10–70 N/m with an oscillation frequency of 250–450 kHz. The samples were dissolved in chloroform to yield 1 w/v% solutions that were slow-cast on clean cover slides. The

Scheme 1 Synthetic route for the preparation of PUUs**Table 1** PUUs formulations, molecular weights, density and water contact angles

Sample	PCL/PEG weight ratio ^a	M_w ($\times 1,000$)	PDI	Contact angle
PUU1	100/0	79	1.210	84 ± 1.0
PUU2	80/20	67	1.503	69 ± 1.2
PUU3	50/50	73	1.480	55 ± 1.0

^a Molar ratio of polyol:isocyanate:benzoic acid in all compounds was 1:2:1

resulting films were dried at room temperature for about 5 h to complete removal of the solvent.

Preparation of PUUs

The PUUs were synthesized using the method reported in literature [19]. Briefly, a mixture of PCL and PEG, at different weight ratios, was used as polyols for the preparation of PUUs. The diols were reacted with HDI (the overall ratio of NCO to OH was kept at 2–1) in a three-necked reaction kettle equipped with mechanical stirrer, heating mantle, reflux condenser, dropping funnel and N_2 inlet and outlet at 85°C . The reaction was continued until the NCO content reached the theoretical value as determined by dibutyl amine titration according to ASTM D 2572. Then, DMSO was added into the reaction kettle to dissolve the prepared isocyanate-terminated prepolymer (ITPP). At this point, an equimolar quantity of benzoic acid (with respect to ITPP), dissolved in excess amount of DMSO, was added and the mixture was allowed to react at 40°C over night to complete conversion of intermediate ITPP to PUU. Scheme 1 outlines the synthetic route for the preparation of PUUs. Different formulations of the polymers are collected in Table 1.

Finally, the polymer solution was precipitated in distilled water and immersed in isopropanol for 24 h to remove unreacted monomers. Eventually, the polymer was dried under vacuum at 50°C for 24 h.

Results and discussion

FTIR spectra of PUU1, PUU2 and PUU3 are illustrated in Fig. 1a. Microphase separation of the segmented PUUs is investigated using two regions of the FTIR spectra. The first region contains three distinct bands between $1,630$ and $1,750\text{ cm}^{-1}$ which is generally known as the carbonyl stretching region (Fig. 1b). In addition to non-hydrogen-bonded urethane and ester carbonyl peaks at $1,735\text{ cm}^{-1}$, the peaks at $1,625$ and $1,660\text{ cm}^{-1}$ represent carbonyl groups that are hydrogen-bonded to either urea N–H groups in an ordered three-dimensional hydrogen bond arrangement (3D H-bond formation between one CO, on one side and two NH groups of the same urea moiety, on the other side), or only one urea or urethane N–H, respectively, in a disordered mode [6]. It may be noted that the, so-called ordered hydrogen bonds are not necessarily involved in crystalline hard domain formation. It is generally believed that in poly(urethane urea)s, a higher degree of microphase separation is observed as the absorbance of the ordered urea CO peak is increased [23].

As it is evident in Fig. 1b, the intensity of the peaks at $1,625$ and $1,660\text{ cm}^{-1}$ follows a decreasing trend from PUU1 to PUU3, because esters contain two electronegative oxygen atoms and the ester carbonyl oxygen is highly polarized and participates in hydrogen bonding. In comparison to the carbonyl oxygen, the ether oxygen exhibits weaker proton affinity and, therefore, acts as a less capable hydrogen bond acceptor (Fig. 1b) [20].

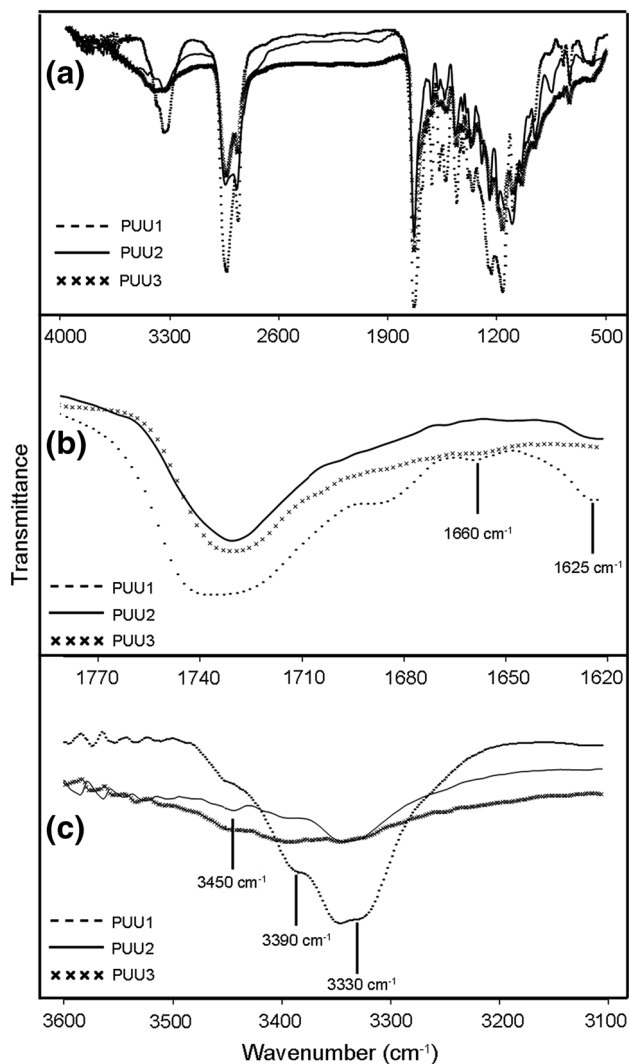


Fig. 1 FTIR spectra of the PUUs **a** full scale, **b** (C=O) stretching region and **c** (N–H) stretching region

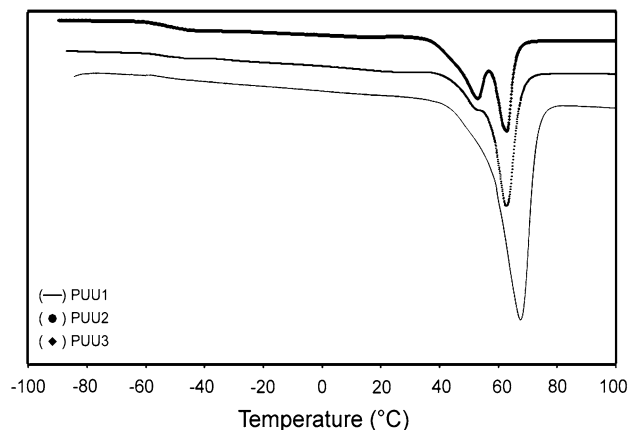


Fig. 2 DSC thermograms of PUU1, PUU2 and PUU3

Table 2 PUUs glass transition temperature, melting point and heat of fusion

Sample	Glass transition (°C) of PCL	Melting point (°C)		Heat of fusion (J/g)	
		PCL	PEG	PCL (Theo./Exp.)	PEG
PUU1	-47	67.4	-	75.5	-
PUU2	-49	64.1	57.6	56.6/52.2	13.7
PUU3	-52	64.5	57.4	37.7/28.4	23.2

Another hydrogen-bonded N–H in both the urethane and the urea units region is located between 3,200 and 3,500 cm^{-1} as shown in Fig. 1c. The peaks related to the stretching mode of the ordered and the disordered hydrogen-bonded N–H groups as well as the non-bonded N–H group have appeared at 3,330, 3,390 and 3,450 cm^{-1} , respectively [6].

The intensity of the peaks regarded as the ordered and the disordered hydrogen-bonded N–H groups is distinctly reduced, as the contribution of the PEG soft segments to the overall PUU structure has been increased. Therefore, the FTIR data indicate that the structure of PUUs moves to significantly less ordered systems with reduced degree of microphase separation in the presence of increasing amounts of PEG soft segments.

The molecular weights, polydispersity and water contact angle of the PUUs are listed in Table 1. The data show that the produced polymers have narrow molecular weights distribution. Also, by increasing PEG percentage content of the PUUs backbone, hydrophilicity and water absorption of the segmented polymers (PUUs) are increased, which may be attributed to the ability of PEG segments to establish hydrogen bonding type interactions with water molecules.

The calorimetry curves of the prepared segmented polymers (PUU1, PUU2 and PUU3) are displayed in Fig. 2. The DSC curve of PUU1 shows two transitions around -50 and 67 $^{\circ}\text{C}$, which are attributed to the glass transition temperature (T_g) and melting temperature (T_m) of the soft segments of PUU1, respectively. By introducing PEG into the backbone of the polymers (PUU2 and PUU3), in addition, a shoulder has appeared at lower edge of the melting peak and the transition related to PCL is slightly shifted to lower temperatures. A close inspection of Fig. 2 reveals that sharpness of the corresponding T_g transition of the soft segment is increased upon PEG addition, which is possibly related to the deformity of PCL segments structural order in the presence of PEG segments. This conclusion is confirmed by the fact that the melting temperature and heat of fusion of PCL segment decrease with increasing the amounts of PEG segment (Table 2).

In Fig. 3a, b, the storage moduli and $\tan \delta$ curves are recorded against temperature for the prepared PUUs. Two

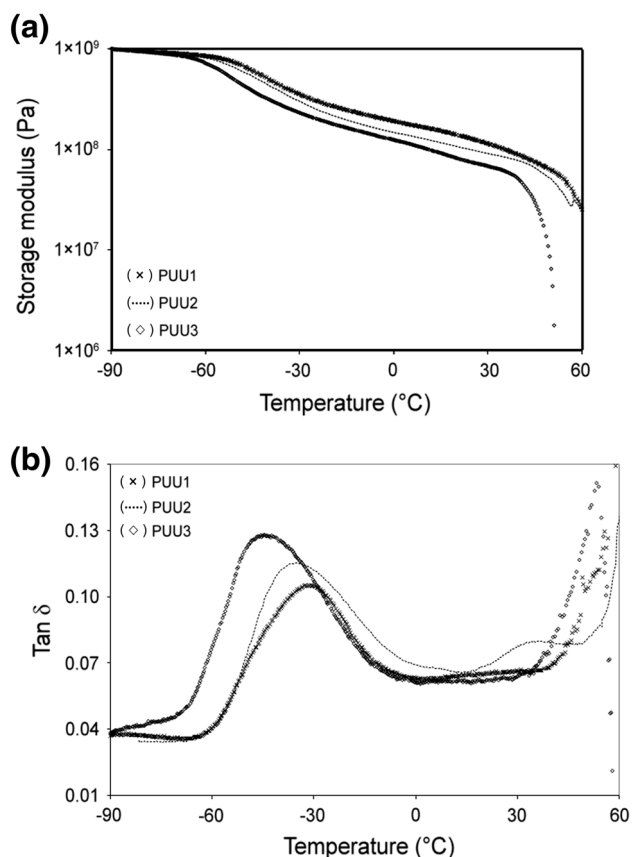


Fig. 3 Storage modulus (E') **a** and $\tan \delta$ **b** curves versus temperature for PUU1, PUU2 and PUU3

transitions at around -45 and 50 $^{\circ}\text{C}$ may be attributed to the glass and melting transitions of the semi-crystalline soft segments in PUUs which have appeared at slightly lower temperatures compared to those found with DSC. These shifts are possibly due to the lower temperature scan rate applied for DMA measurements. As it can be seen in Fig. 3a, b, increase in the amount of PEG has led to a sudden drop in T_g : a change which is in good agreement with DSC results. For PUU1, the decrease in storage modulus after the first transition is about one order of magnitude, which is most possibly due to the high physical cross-linking of this sample [7]. Also, above the corresponding T_g of PUU1, the rubbery plateau exhibits a high storage modulus of slightly above 10^8 Pa. This high modulus value indicates the presence of long-range connectivity of the hard segment and percolation of the hard phase through the soft matrix [14]. This value decreases by increasing the PEG content. Moreover, noticeable reductions in the modulus of the rubbery plateau are observed from PUU1 to PUU3. The decrease is possibly because of weaker hydrogen bonding within the hard segments of PCL/PEG PUUs as it is indicated by FTIR spectroscopy data.

Mechanical properties of the PUUs were examined through strain–stress measurements in tensile mode

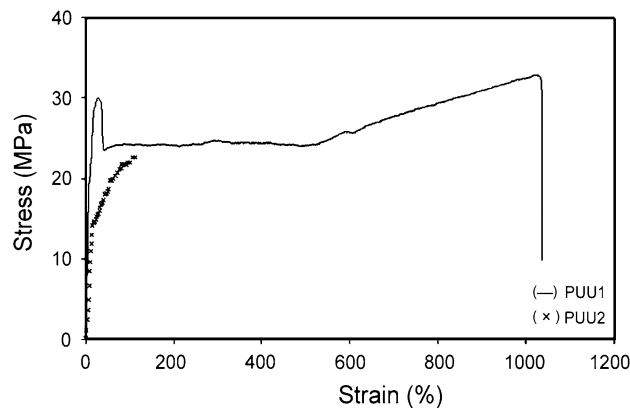


Fig. 4 The stress–strain curves of the PUUs

(Fig. 4). It can be seen that, by introducing PEG moieties, thermoplastic characteristics of the polymer turn to brittle behavior; therefore, tensile test analysis was not possible on PUU3 (PCL/PEG = 1) sample. PUU1 shows higher elongation with a strain-at-break of about 1,250 %. However, with inclusion of PEG into PUU formulation, the tensile strain is decreased. This is due to weaker inter-chain interactions between the polyether chains compared to polyesters which generally lead to PUs with inferior mechanical properties. This phenomenon is often attributed to stronger hydrogen bonding between the NH and the ester carbonyl group, rather than urethane NH-ether oxygen H-bonds (about 40 % of the polyether urethane carbonyl groups are hydrogen bonded in comparison with polyester urethane carbonyl of the same hard segment content). Furthermore, it is supposed that strong ester bonds of PCL are non-rotating, whereas PEG has a relatively weak ether bond which undergoes free rotation. Therefore, PEG with its brittle nature is considered a feeble material and presumably the variation (observed reduction) in the mechanical properties is due to PEG inclusion [24, 25].

Previously, Wagner et al. compared the mechanical properties of poly(ether ester urethane)urea based on poly(ether ester) tri-block copolymers (PCL–PEG–PCL) with poly(ester urethane)urea (PCL-based PUU, of the same hard segment chemical structure), and concluded that the incorporation of PEG into the soft segment resulted in reduced initial modulus, tensile strength and breaking strain [22].

Microphase separation between the hard and the soft domains of the synthesized PUUs was studied using AFM in tapping mode. The AFM phase images of PUUs are shown in Fig. 5a–c. The observed contrast in the figures originates from the microphase separation between the hard and soft domains within the films which is well documented for PUs and polyureas. The bright dispersed regions of higher modulus correspond to hard domains and the dark areas correspond to the soft segment matrix. The

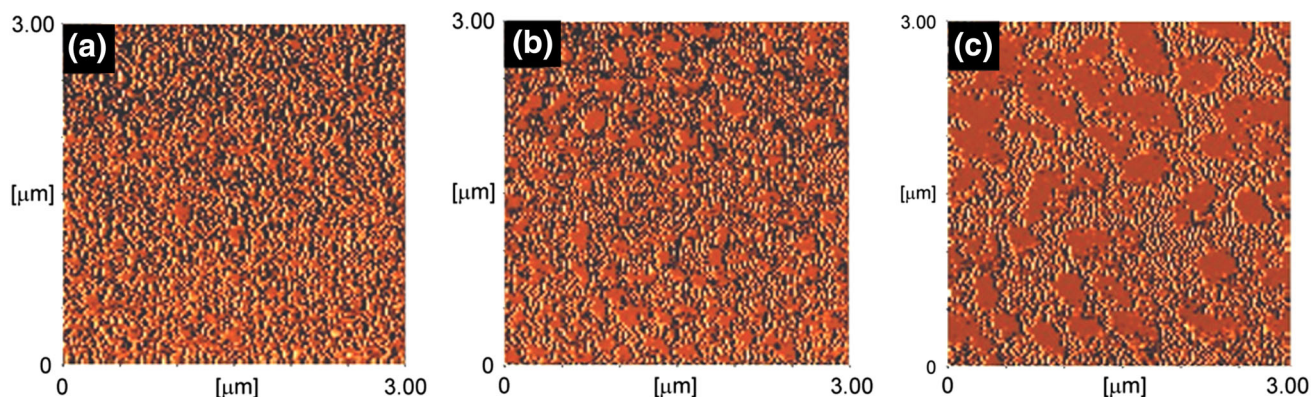


Fig. 5 AFM tapping mode phase images of the PUUs **a** PUU1, **b** PUU2 and **c** PUU3. The scan size of all images was $3 \times 3 \mu\text{m}$

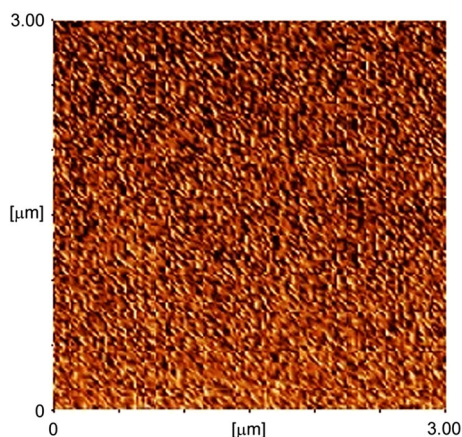


Fig. 6 AFM tapping mode phase images of heat-treated PUU1

figures show that the hard blocks are embedded in a soft matrix in all polymers. Continuity of the hard microdomains, dispersed in PCL phase soft segments, is clearly observed in Fig. 5a. As it can be seen in the figure, the hard segments in PUU1 seem to be distributed homogeneously into the soft segments and form interconnected short domains, which are linked through many narrow bridges

which are almost uniformly scattered within the soft segment phase. By PEG content increases, hard segment-rich areas are formed and as it can be seen in Fig. 5a–c distinction between the light and the dark (soft segments) regions becomes more pronounced. These interconnected areas can be explained as agglomerations of delicate domains of hard segments. Since hydrogen bonds act as physical cross-links in PUU1, the hard segment domains are distributed regularly in the sample. Hard segment in polyether/ester-based PUUs is built up of fine nano-domains inhomogeneously distributed in the whole sample. Therefore, it may be said that in the polyester polyol based PUU there is stronger interaction between the hard and soft segments and as a result the formation of regularly dispersed particles of the hard phase is clearly evident, while, it is not so with a polyether/ester-based PUUs, when even the hard segment content is kept constant. This phenomenon is attributed to higher density of hydrogen bonding in PCL-based PUU and thus, more integration of hard domains would occur in the polymer in absence of PEG, which is in line with the results obtained by FTIR.

The existence of hydrogen bonds exclusively within the hard segment domains causes phase segregation to a greater extent. On the other hand, formation of inter-phase

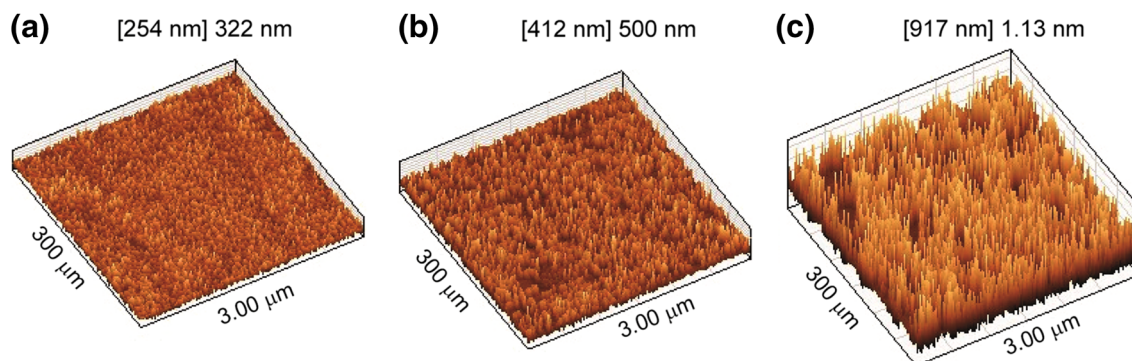


Fig. 7 AFM 3D topography of **a** PUU1, **b** PUU2 and **c** PUU3

hydrogen bonding (between the soft and hard segments) induces an enhanced degree of phase mixing. Also, the strong intermolecular interaction arising from hydrogen bonding establishes a primary driving force for microphase separation.

To provide evidence to confirm the light areas as the hard segments, merely, PUU1 was heated at 80 °C (significantly above the melting temperatures of both polyols), for 15 min to melt the soft phase crystals. Then, it was followed by quenching the sample in liquid nitrogen. AFM observation of this heat-treated sample in comparison with the prepared PUU1 revealed that the phase structure remains almost intact upon heat treatment (Fig. 6).

Surface roughness of the segmented PUUs films is shown in Fig. 7. As it can be seen, PUU1 based on PCL has produced a smooth surface film and by inclusion of PEG in the structure of PCL-based PUU, the surface roughness of the film is increased significantly.

Conclusion

Aiming to take control over the PUUs hydrophilicity, the polymers based on mixed polyols systems (PCL/PEG) were synthesized. The morphology and microphase separation of PCL/PEG-based thermoplastic PUUs were investigated as a function of their soft segment composition. FTIR, DSC, DMA, tensile measurement and AFM were used to visualize the changes in the microphase-separated structure of the segmented PUUs. The results showed that although the covalent cross-link network is definitely expected to play a controlling role in imparting mechanical robustness to materials, the physically cross-linked network also plays a determining role in PUs bulk properties and mechanical properties in particular. Since an aptly balanced inter-relationship was shown between PEG, the microstructure and the PUUs polymers bulk properties, it can be concluded that hydrogen bonding (as the driving force of the observed differences between PUUs) within the hard domains can be modulated by the soft segment compositions.

References

1. Wu L, You B, Li D, Qian F (2000) The in vitro and in vivo stability of poly(urethane urea)s as biomedical materials. *Polym Degrad Stab* 70:65–69
2. Hong Y, Guan J, Fujimoto KL, Hashizume L, Pelinescu AL, Wagner WR (2010) Tailoring the degradation kinetics of poly(ester carbonate urethane)urea thermoplastic elastomers for tissue engineering scaffolds. *Biomaterials* 31:4249–4258
3. Wang F, Li Z, Lannutti JL, Wagner WR, Guan J (2009) Synthesis, characterization and surface modification of low moduli poly(ether carbonate urethane)ureas for soft tissue engineering. *Acta Biomater* 5:2901–2912
4. Hood MA, Wang B, Sands JM, La Scala JJ, Beyer FL, Li CY (2010) Morphology control of segmented polyurethanes by crystallization of hard and soft segments. *Polymer* 51:2191–2198
5. Wang CB, Cooper SL (1983) Morphology and properties of segmented polyether polyurethane ureas. *Macromolecules* 16:775–786
6. Christenson EM, Anderson JM, Hiltner A, Baer E (2005) Relationship between nano-scale deformation processes and elastic behavior of polyurethane elastomers. *Polymer* 46:11744–11754
7. Bagdi K, Molnár K, Sajó I, Pukánszky B (2011) Specific interactions, structure and properties in segmented polyurethane elastomers. *Express Polym Lett* 5:417–427
8. Shokrollahi P, Mirzadeh H, Huck WTS, Scherman QA (2010) Effect of self-complementary motifs on phase compatibility and material properties in blends of supramolecular polymers. *Polymer* 51:6303–6312
9. Garrett JT, Xu R, Cho J, Runt J (2003) Phase separation of diamine chain-extended poly(urethane) copolymers: FTIR spectroscopy and phase transitions. *Polymer* 44:2711–2719
10. Wisse E, Spiering AJH, van Leeuwen ENM, Renken RAE, Dankers PYW, Brouwer LA, van Luyn MJA, Harmsen MC, Sommerdijk NAJM, Meijer EW (2006) Molecular recognition in poly(ϵ -caprolactone)-based thermoplastic elastomers. *Biomacromolecules* 7:3385–3395
11. Pongkitwitton S, Hernández R, Weksler J, Padsalgikar A, Choi T, Runt J (2009) Temperature dependent micro-phase mixing of model polyurethanes with different inter-segment compatibilities. *Polymer* 50:6305–6311
12. Huang SL, Chao MS, Ruaan RC, Lai JY (2000) Micro-phase separated structure and protein adsorption of polyurethanes with butadiene soft segment. *Eur Polym J* 36:285–294
13. Pergal MV, Džunuzovic JV, Poreba R, Ostojic S, Radulovic A, Špirková M (2013) Microstructure and properties of poly(urethane-siloxane)s based on hyperbranched polyester of the fourth pseudo generation. *Prog Org Coat* 76:743–749
14. O'Sickey MJ, Lawrey BD, Wilks JL (2002) Structure–property relationships of poly(urethane urea)s with ultra-low monol content poly(propylene glycol) soft segments. I. Influence of soft segment molecular weight and hard segment content. *J Appl Polym Sci* 84:229–243
15. Eceiza A, Larranaga M, de la Caba K, Kortaberria G, Marieta C, Corcuera MA, Mondragon I (2008) Structure–property relationships of thermoplastic polyurethane elastomers based on polycarbonate diols. *J Appl Polym Sci* 108:3092–3103
16. Gisselalt K, Helgee B (2003) Effect of soft segment length and chain extender structure on phase separation and morphology in poly(urethane urea)s. *Macromol Mater Eng* 288:265–271
17. Sheth JP, Unal S, Yilgor E, Yilgor I, Beyer FL, Long TE, Wilkes GL (2005) A comparative study of the structure–property behavior of highly branched segmented poly(urethane urea) copolymers and their linear analogs. *Polymer* 46:10180–10190
18. Dasa S, Cox DF, Wilkes GL, Klinedinst DB, Yilgor I, Yilgor E, Beyer FL (2007) Effect of symmetry and H-bond strength of hard segments on the structure property relationships of segmented, nonchain extended polyurethanes and polyureas. *J Macromol Sci B* 46:853–875
19. Shokrollahi F, Yeganeh H, Mirzadeh H (2011) Simple and versatile method for the one-pot synthesis of segmented poly(urethane urea)s via in situ-formed AB-type macromonomers. *Polym Int* 60:620–629
20. Guelcher SA (2008) Biodegradable polyurethanes: synthesis and applications in regenerative medicine. *Tissue Eng Part B* 14:3–17
21. Gorna K, Gogolewski S (2002) Biodegradable polyurethanes for implants. II. In vitro degradation and calcification of materials from poly(ϵ -caprolactone)-poly(ethylene oxide) diols and various chain extenders. *J Biomed Mater Res* 60:592–606

22. Guan J, Sacks MS, Beckman EJ, Wagner WR (2004) Biodegradable poly(ether ester urethane)urea elastomers based on poly(ether ester) triblock copolymers and putrescine: synthesis, characterization and cytocompatibility. *Biomaterials* 25:85–96
23. Luo N, Wang DN, Ying SK (1996) Hydrogen bonding between urethane and urea: band assignment for the carbonyl region of FTIR spectrum. *Polymer* 37:3045–3047
24. Scerba MT, DeBlase AF, Bloom S, Dudding T, Johnson MA, Lectka T (2012) Characterization of highly unusual $\text{NH}^+\text{-O}$ hydrogen bonding to ester ether oxygen atoms through spectroscopic and computational studies. *J Phys Chem A* 116:3556–3560
25. Sheth JP, Klinedinst DB, Wilkes GL, Yilgor I, Yilgor E (2005) Role of chain symmetry and hydrogen bonding in segmented copolymers with monodisperse hard segments. *Polymer* 46:7317–7322